PLASTICS TESTING

1. Introduction

Plastics testing encompasses the entire range of polymeric material characterizations, from structure to material response to environmental effects. Whether the analysis or property testing is for quality control of an industrial plastic or for the determination of the relaxation response of a material to an imposed stress, a variety of test techniques is available for the researcher (see CHARACTERIZATION OF POLYMERS).

Polymer analysis continues to progress with improvements in instrumental techniques and computer-enhanced data analysis methods that allow detection of effects of side-chain rotations or localized variation in free volume of a polymer film. Combinations of instrumental analysis techniques such as pyrolysis–gas chromatography (pyrolysis–GC) or liquid chromatography–mass spectroscopy (LC–MS), used for separation and identification of polymer components and degradation products from complex systems have been further enhanced with the addition of thermal techniques that allow targeting narrow temperature ranges or microscopy techniques targeting localized areas of a sample for analysis. (see MASS SPECTROMETRY; CHROMATOGRAPHY, HPLC; CHROMATOGRAPHY, SIZE EXCLUSION). Atomic Force Microscopy (AFM) allows determination of polymer Morphology at the nano level. The use of microprocessors to capture transient signals from physical test methods, ie high speed impact, allows the observation of the complete impact event, while improvements in fracture mechanics techniques lead to increased understanding of material response to stress independent of geometry effects.

2. Composition and Structure

Fourier transform infrared (FTIR) is one of the most commonly used analysis methods for determining the composition of polymers (see VIBRATIONAL SPECTROSCOPY). Other routine applications are in fingerprinting contaminants, characterizing chemical property gradients, or mapping physical property anisotropy (1). The FTIR technique, which corresponds to the vibrational energies of atoms or specific groups of atoms within a molecule as well as rotational energies, identifies components by comparing the spectrum of a sample to reference spectra. The infrared spectral region is commonly from 2 to 50 μm, and the region of 7–15 μm is capable of differentiating similar isomers (2). The 7–8.5-μm region has been used in model hydrocarbon studies to show that the absorption of methylene groups is dependent on the size of the methylene sequences in compounds (3). FTIR has been used to study structural modifications of polypropylene during aging (4), determine crystalline forms of syndiotatic polystyrene through spectral subtraction methods (5), simultaneously monitor polymerization and microphase separation in a polyurethane system through identification of reaction products formed (6), and to quantitate grafting levels of succinic anhydride onto polypropylene (7).

Some examples of composition determinations using IR analysis of polymers are as follows. The N stretching mode has been used for quantitative

analysis of acrylonitrile in butadiene–acrylonitrile copolymers (8). [Residual catalyst support in commercial polyethylene can be detected at levels as low as 100 ppm (9)]. The short-chain branching distribution of an ethylene 1-olefin copolymer across the molecular weight distribution was determined using a combination of size exclusion chromatography (SEC) with FTIR (10). There are several excellent sources of spectra both in print and on computer disk for comparing and matching the fingerprints obtained from a sample (11,12).

Tracking of trans conformers in sub-T_g annealed amorphous poly(ethylene terephthalate) (PET) films by FTIR indicated that closer interchain packing and formation of new cohesional entanglements along the chains occur that are not apparent in quenched or slowly cooled material (13). Step-scan FTIR photoacoustic analysis was used in determining surface stratification of components within a thermoplastic olefin. The IR bands were used as analytical depth-profiling probes to establish the orgin of photoacoustic (PA) signals (14). FTIR monitoring of the stress relaxation of polyurethanes led to the determination that differences in phase separation was related to the structure of the polymer (15). The combination of FTIR with *in situ* WAXS (wide-angle X-ray spectroscopy (qv)) measurements during the drawing and annealing of PET film allowed the study of the development of molecular orientation and crystallization (16). Specular reflectance FTIR–microscopy has been used in studies of several polymers: liquid crystalline polymers, side-chaiin (LCP) (17,18), polyurethanes (19), carbon-filled polymers (20,21), and poly(aryl ether ether ketone) (PEEK) (1). Progress has been made in the development of on-line IR equipment for monitoring the extrusion of polymers using the near-IR range rather than mid-IR with resultant lower sensitivity to molecular fragments (22). Some work has been done on calibration of these systems against dynamic rheological standards (23). Real-time quantitative monitoring of the level of filler in extruded polymers has been reported using near-IR spectroscopy (24).

Combination techniques such as microscopy–FTIR and pyrolysis–IR have helped solve some particularly difficult separations and complex identifications. Microscopy–FTIR has been used to determine the composition of copolymer fibers (25); polyacrylonitrile, methyl acrylate, and a dye-receptive organic sulfonate trimer have been identified in acrylic fiber. Both normal and grazing angle modes can be used to identify components (1–7). Pyrolysis–IR has been used to study polymer decomposition (27).

Raman spectroscopy is an emission phenomenon as opposed to IR absorption, and results from vibrations caused by changes in polarizability (see VIBRATIONAL SPECTROSCOPY). Raman spectroscopy had limited use until the advent of lasers as the exciting source. It can be complementary to IR and may be more useful when the sample for analysis is a filled polymer or composite containing silica, clay, other similar inorganic filler, or a piece of polymer, but particularly thermosets or rubbery products requiring no further sample preparation. Additional advantages over IR are the intensity advantage for the C=C band and the determination of thiol groups in sulfur polymers (28). Fluorescence is a significant interference in Raman spectroscopy because it occurs simultaneously in several commercial plastic products. Fourier transform of Raman spectroscopy and other techniques for reducing fluoresence (29,30) have expanded its applicability. FT-Raman spectroscopy has been used as an alternative technique to

thermal gravimetric analysis (TGA) of filler content up to 75 wt% of the polymer (1). It has also been used to determine the isotacticity of polypropylene giving good correlation to FTIR and ^{13}C NMR data (31).

Studies of blends using Raman imaging and Raman microscopy have been used to determine miscibility and phase behavior of blends (32) and morphology in blends of linear and branched polyethylene (33). On-line Raman was used to monitor copolymerization of styrene and *n*-butyl acrylate by monitoring monomer concentrations (34). Raman longitude acoustical mode (LAM) was used to study stress-induced states of a blend of polyethylenes in a microfilm. Structure appeared to be the formation of straight tie molecules localized in neighboring crystals with amorphous layers between the crystals. Presence of all-trans sequences with length exceeding the mean crystallite size appeared to be due to stress-induced gauche to trans formations in the amorphous phase (35).

Nuclear magnetic resonance (NMR) requires an atomic nucleus that can absorb a radio-frequency signal impinging it in a strong magnetic field to give a spectrum. The field strength at which the nucleus absorbs is a function of both the nucleus and its immediate electronic environment. The atoms normally used for NMR analysis are as follows (36): ^{1}H, ^{19}F, ^{31}P, ^{11}B, ^{14}N, ^{29}Si, ^{13}C, ^{2}H, ^{17}O, ^{33}S, and ^{15}N. Of these, the most commonly used in polymer analyses are ^{1}H and ^{13}C. Solid-state ^{13}C NMR utilizing proton spin-lattice relaxation time in the rotating frame has been used for determination of composition, phase, and compatibility (misciblity) of blends (37–40). In combination with SEC, ^{13}C NMR is capable of quantitating both long- and short-chain branching in polymers (41). The technique has also been used for characterizing molecular structure differences in reject ethylene vinyl alcohol polymer that correlated to changes in thermal and mechanical properties (42). A combination of ^{13}C NMR and deuterium NMR were used to determine the effects of low molecular weight additives on secondary relaxation processes in PET. The additives were found to reduce the number of phenyl ring flips that were shown by the deuterium NMR to closely relate to the relaxation peak observed by dynamic mechanical thermal analysis (43). Fourier transform has also been applied to NMR, allowing increased sensitivity on microsamples. Spectra can be obtained on as little as 10 μg (44). NMR techniques were used to study the reactions and catalytic activity of different agents for transesterification reactions between polymers (45). Two-dimensional time-domain proton NMR identified and characterized relaxation components over a temperature range. Phase transitions and different phases were observed (46). Similar analysis of high density polyethylene (HDPE) showed three phases, which have been tentatively identified as a crystalline region, an area of chain loops on the surface of crystallites and entangled chain segments, and the third phase of chains in the amorphous phase (47). Molecular chain dynamics, chain orientation, and molecular packing differences were determined in HDPE and isotactic polypropylene (48). Microphase separation in polyureas that were prepared by RIM (reaction injection molding) techniques were determined with solid-state NMR (49).

An additional technique that has been found useful in analysis of the composition of polymers and blends is liquid chromatography. Pasch and Rode used the critical point of adsorption of the least polar component of a blend to determine the liquid chromatographic conditions for separating blends of

polymethacrylates into components (50). High pressure liquid chromatography (HPLC) in combination with mass spectroscopy was used to analyze the components of an epoxy resin (51). HPLC has also been used with a precipitation–redissolution technique to separate polymer molecular weights for several polymers as a shorter technique compared to SEC (52). Reverse-phase liquid chromatography with UV detection was useful in qualitative determination of brominated flame retardants in polymeric waste materials (53).

Pyrolysis techniques for thermally degrading polymers have high sensitivity, allow trace analysis of all organics in liquid or solid state, require minimal sample preparation and small amounts of sample, and allow simultaneous identification and quantification in one run. However, they may have limited reproducibility and limited applicability where inorganic fillers are present (54). There have been various types of pre- and post-pyrolysis derivations done to simplify analysis by GC separation and reduce interferences from surrounding materials (55).

Many studies have been published on the use of pyrolysis–GC: Determination of the primary degradation products of polyacrylonitrile (56), number-average molecular mass using end-group analysis (57), kinetic measurements of the thermal degradation of polymers using sequential pyrolysis (58), determination of stereospecific sequencing in polypropylene (59), composition and microstructure of styrene maleic anhydride (SMA) copolymers (60) are examples in addition to frequent use in determination of additives. Combinations of pyrolysis–GC with FTIR techniques have been used in the characterization of branching in comb-like polymers (61) and analysis of butadiene–acrylonitrile copolymers (62). Additional examples of use of pyrolysis–GC for polymer systems can be found in Wampler's (63) and Bart's (54) reviews.

Additives to polymers are important components affecting the polymer's performance in processing, aging, and maintaining properties under adverse environmental conditions. In some cases it is possible to determine these in solid or molten polymer, but generally they must be separated from the polymer prior to analysis. Typical methods that have been used for obtaining a sample for additives analysis include solvent extracting, dissolving the polymer matrix, hydrolyzing the material, or thermally destroying the matrix. Samples are then analyzed using gas or liquid chromatography techniques alone or in combination with mass spectroscopy to identify specific components. pyrolysis–GC has been shown to be particularly useful for analysis of flame retardants (64,65), plasticizers (66), lubricants (67), antioxidants (68), and other stabilizers (69,70) in many polymer matrices. Figure 1 gives a pyrogram of a common lubricant, ethylenebistearamide.

Various techniques for extracting and analyzing low molecular weight components of polymers include static and dynamic heat extractions, headspace analysis, and thermochromatography (71). These are used primarily where solventless systems are required for analysis (72,73). Gas-phase mirage-effect spectroscopy has been used for measuring trace gases and organic volatiles up to parts per billion (ppb) levels during nondestructive characterization and photodecomposition studies (74). Packed column supercritical fluid chromatography (pSFC) with atmospheric pressure chemical ionization detection has been

shown to detect and quantitate a variety of additives, including antioxidants, light stabilizers, and slip agents (75).

New technologies in the area of microscopy, such as atomic force microscopy (AFM) and electron spin resonance (ESR), have allowed the study of morphology of polymers and blends of polymers to extend to localized areas at interfaces of phases in semicrystalline polymers. Other techniques such as wide-angle and small-angle X-ray scattering (WAXS, SAXS), small-angle neutron scattering (SANS), small-angle light scattering (SALS), scanning and transmission electron microscopy (SEM, TEM) have been used for structure studies as well. WAXS has been used for examining the crystalline regions of semicrystalline polymers and composites (76–78). SAXS was used with linear correlation functions to determine the overall crystallinity and fraction of semicrystalline stacks during crystallization and melting of linear polyethylene (79) while crystallite size distributions were calculated from WAXS profiles in a similar polymer (80). By monitoring the surface structure of a PEEK composite, skin effects were observed using reflectance WAXS (81). SAXS allows the determination of morphology via domains and microstructure by varying electron density in different areas of a material or density differences between amorphous and crystalline phases (82,83). This has been shown to be useful in determining the phase behavior of blends of poly(vinyl methyl ether) with styrene–butadiene–styrene copolymers (84). Correlation of thermal and structural properties of a blend of polyamide with liquid crystal polymer over a range of compositions and thermal treatments (85) and determination of an ordered crystalline/amorphous lamellar structure in a blend of poly(ethylene oxide) and poly(vinyl acetate) (86) have used SAXS. This technique has also been used qualitatively in determining domains and component mixing with interpenetrating polymer networks (87). Other X-ray techniques were used to show the solid-state structures of aromatic copolyesters (88) and measure crystalline form transition under stress with poly(butylene terephthalate) (89).

Structure determinations in polymers have involved the use of SANS techniques to evaluate not only the radius of polymer molecule gyration where light or X-ray scattering is not usable, but also phase dimensions in multicomponent polymers and suggested mechanisms of phase separation (90). Applications in polymer melts as well as concentrated and dilute solutions of polymers and solid-state samples have investigated the nature of semicrystalline polymers, polymer blends, and the development of new theories of polymer solutions and networks (91). Another technique finding use in structure analysis is dielectric spectroscopy. A combination of X-ray scattering and dielectric spectroscopy has been used to study the noncrystalline regions of semicrystalline polymers; this technique uses semicrystalline and amorphous polymer blends in which the amorphous polymer, although miscible in amorphous regions, is excluded from the crystal–amorphous interphase region (92). SALS techniques have been able to distinguish between nucleation and growth and spinodal decomposition in phase separation mechanisms (93). SEM has been used to determine the location of compatibilizers at the interface of blends of thermoplastic urethanes and polypropylene (94).

AFM is used at the nanoscale to analyze structure of polymers. It has been used to determine spatial distribution of impact modifier in high impact

polypropylene (95), follow pit growth in a film of a blend as a function of exposure time during degradation studies of coatings on metal (96), determine surface topography and molecular organization of liquid crystalline polymers (97), and observe nanoparticles in polypropylene matrix (98). In combination with other techniques it allows the determination of composition versus depth of nano silica particles in a surface film, including the location of sub-surface nano silica particles (99). AFM in conjunction with SEM was used to study the influence of aging on morphology of polypyrrole films (100). The use of a vibrating, heating stage for mounting samples and observing the effects on the AFM cantilever allows the study of local elastic and viscoelastic properties (101). Figure 2 shows both topography and simultaneously acquired amplitude images with this technique. Scanning force microscopy of isotatic polypropylene under a moderate applied shear stress was used to study plasticity and damage mechanisms (102).

ESR techniques use nitroxyl radicals either dispersed in polymer matrix (spin probe) or covalently bonded to polymer chain (spin label) which are sensitive to the environment allowing molecular motion and microstructure of polymers to be identified from spectra (103). Quantitative methods of heterogeneous ESR spectra are divided into (*1*) outer hyperfine etrema, (*2*) signal intensities related to the relative concentration of the probe in different phases, and (*3*) simulation of the spectra. The presence of two well-separated outer maxima above the glass-transition temperature could be ascribed to two phases in natural rubber (104), miscible blends (105), immiscible blends (106), cross-linked polymers (107), and polyurethanes (108). ESR has used the measurement of the oxidation product to monitor the consumption of stabilizer in polypropylene (109).

3. Molecular Weight

The molecular weight and the distribution of multiple molecular weights normally found within a commercial polymer influence both the processibility of the material and its mechanical properties. For a few well-defined homopolymers, an analysis of composition and molecular weight is sufficient to define the likely mechanical of the polymer.

Low-angle laser light scattering (turbidity) has been found to be the most accurate and reproducible technique for measuring polymer molecular weights (average molecular weight) as a primary method (110) (see MOLECULAR WEIGHT DETERMINATION). Most turbidimetric techniques use polymer solubility as a function of temperature for defining molecular weights (111). Dynamic light scattering has been used to obtain the distribution of hydrodynamic radius, which can be converted to molecular weight distribution with appropriate calibration. This technique can be performed in corrosive solvents or with polymers that dissolve only at high temperatures (112). Gel-permeation chromatography (GPC), although a secondary technique requiring careful calibration and interpretation of data, is the most frequently used commercial technique because of its ease of use, low cost, short time for analysis, and generation of excellent comparative data (113). Shifting of the polymer molecular weight peak or displacement in

comparison to a standard or good material can indicate the presence of a higher molecular weight species by showing a shift to early elution, or a lower molecular weight species by showing a shift to later elution. These shifts can affect the processibility and physical performance of the material. Small sharp peaks that elute late from the GPC column may indicate the presence of low molecular weight oligomers, residual monomers, additives, or even residual moisture in the polymer.

A wide variety of polymers have been analyzed by gel-permeation or chromatography, size exclusion (SEC) to determine molecular weight distribution of the polymer and additives (114–117). Improvements in GPC include smaller cross-linked polystyrene beads having narrow particle size distributions, which allow higher column efficiency and new families of porous hydrophilic gels to be used for aqueous GPC (118). SEC in combination with FTIR has been used to monitor component content and compositional effects with changes in molar mass of HDPE and polypropylene (119). SEC fractionation followed by NMR and multiangle light scattering detector (MALDI) of random copolymers of acrylates with styrene maleic anhydride allowed determination of a model for composition and the ratio between number-average molecular weight (M_n) and weight-average molecular weight (M_w) of the SEC fraction (120). The combination of SEC with MALDI was also used to characterize branched polystyrene and poly(benzyl methacrylate) (121,122).

Temperature-rising elution fractionation (TREF) is a technique for obtaining fractions based on crystallizability independent of molecular weight effects (123,124) which allows qualitative analysis of short-chain branching in olefins. Determination of crystallizable lengths from TREF spectra led to the development of a quantitative method for short-chain branching (125). Single-step crystallization fractionation (CRYSTAF) has been developed for measuring composition or short-chain branching distribution by monitoring on-line polymer concentration in solution at decreasing temperatures (124). TREF, CRYSTAF, and differential scanning calorimetery (DSC) with specialized sample preparation were used to determine short-chain branching distribution and composition of blends of linear low density polyethylene (LLDPE). All three methods showed similar comonomer distribution (125) (see Fig. 3). Characterization of HDPE chain structure with SEC and CRYSTAF methods was able to be correlated to environmental stress-crack resistance (126).

.

4. Thermal Properties

Thermal analysis involves techniques in which a physical property of a material is measured against temperature at the same time the material is exposed to a controlled temperature program. A wide range of thermal analysis techniques have been developed since the commercial development of automated thermal equipment as listed in Table 1. Of these the best known and most often used for polymers are thermogravimetry (TG), differential thermal analysis (DTA), differential scanning calorimetry (DSC), and dynamic mechanical analysis (DMA).

Thermogravimetric analysis (TGA), which monitors the change in the mass of a material during a controlled temperature ramp, is useful for both qualitative and quantitative analysis. It is used to help identify the types of polymers by comparison to degradation curves or when used with FTIR or pyrolysis–GC-MS (128–132), as well as identify and quantify additives such as carbon fillers, mineral fillers, plasticizers, antioxidants, stabilizers, UV absorbers, nucleating agents, and lubricants (133,134). Carbon black or graphite, which is commonly used as a colorant or filler in many plastics, may be analyzed using TGA by running the analysis in a nitrogen atmosphere to 600°C for measurement of the polymer component and then switching to an oxygen atmosphere and heating to 800 or 900°C to oxidize the carbon (133). The derivative curve of TGA can be used to improve the determinations of onset and end point of decomposition of low level components or in multipolymer systems (135). Refinements in computer control and instrument design have also led to commercial instruments having smooth changes in dynamic heating rate that varies as a function of weight loss, a low mass furnace for rapid response, and horizontal purge gas flow to better remove decomposition products, among other changes (136).

Differential thermal analysis (DTA) monitors the temperature difference between a specimen and a reference material, whereas differential scanning calorimetry (DSC) heats specimen and reference materials separately and measures the heat flow between the materials. DSC is the method of choice for determinations of melting point as well as the presence and level of crystalline phase in polymers. The effects of heating rate and oxygen flow rate on oxidative induction time of HDPE (137), applied strain during cooling (138), spherulitic crystal growth and crystalline structures (139,140), and curing of thermosets (141–143) have been studied using DSC techniques.

DSC has been found suitable for the determination of second-order transitions (T_g = glass transition) and, in some cases, β-transitions. Procedures for the determination of T_g are discussed in the literature (135,136), which includes data on the dependence of T_g on number-average molecular weight (M_n for polymers. This shows a significant effect until a critical M_n is reached with little or no effect beyond. A technique employing DSC to measure specific heat of rapidly quenched polyethylene samples, which are subsequently annealed at low temperatures, shows the formation of secondary crystals that melt near the annealing temperature with small endotherms. The endotherms increase and melting points rise as time increases, leading to the potential use of this technique for studying the thermal history of samples (144,145). Additional work on the correlation of enthalpy changes with the aging of samples has been completed on PBT (146). For amorphous polymers, changes in T_g can be used to determine aging that has occurred below and near T_g. Accuracy is improved by matching the heating rates of DSC to cooling rates on specimen preparation (135,136). The T_g response to aging relates to the continued relaxation of frozen molecular structure that continues over time below T_g and results in changes in free volume (147). Reduction in free volume due to aging can be correlated to reduced impact strength and improved creep response at low strain rates for polymers.

The relative effectiveness of nucleating agents in a polymer can be determined by measuring recrystallization exotherms of samples molded at different temperatures (135). Effects of formulation change on the heat of rubber

vulcanization can be determined by DSC; pressurized cells may be needed to reduce volatilization during the cure process (148).

Changes in heat capacity and measurement of T_g for blends have been used to determine components of copolymers and blends (149–152) although dynamic mechanical analysis has been found to give better resolution. Equations relating T_g of miscible blends and ratios of components have been developed from DSC techniques, eg, the Fox equation (eq. 1), where T_{g12} is the T_g of the blend, W_1 or W_2 is the weight fraction of component 1 or 2, and T_{g1} or T_{g2} is the T_g of the pure component 1 or 2 (153); the Gordon–Taylor–Wood (GTW) equation (eq. 2), where k is the best fit constant for empirical data (154); and the Couchman equation (eq. 3), where x_1 and x_2 are mass fractions and ΔC_p is heat capacity changes for neat polymers (155).

$$\frac{-1}{T_{g12}} = \frac{W_1}{T_{g1}} + \frac{W_2}{T_{g2}} \tag{1}$$

$$\mathrm{T_{g12}} = \frac{k(\mathrm{T_{g2}} - \mathrm{T_g})\mathrm{W_2}}{1 - \mathrm{W_2}} + \mathrm{T_{g1}} \tag{2}$$

$$\ln \mathrm{T_{g12}} = \frac{x_1 \Delta C_{p1} \ln \mathrm{T_{g1}} x_2 \Delta C_{p2} \ln \mathrm{T_{g2}}}{x_1 \Delta C_{p1} + x_2 \Delta C_{p2}} \tag{3}$$

Modulated DSC has been used to evaluate correlations between polymer chain molecular characteristics and crystallization behavior in polyethylene (156). It has also been used in the study of thermal treatments of PET (157) and the kinetics of the T_g (158).

Thermomechanical analysis (TMA) measures the dimensional changes of a fabricated polymer part at a constant heating rate. First-order (T_m) and second-order (T_g) transitions may be measured from graphing length of specimen (L) versus temperature (T). This technique may also be used to determine the coefficient of linear thermal expansion (CLTE) for a material. TMA can be more sensitive to small changes in enthalpy typical of highly crystalline polymers than DSC (159). This technique has also been used for evaluating dimensional changes of polymers in fluid environments. Studies have been completed on water–nylon 6 at different temperatures (160), chlorobenzene–polyethylene (161), and elastomers in various fluid and oils.

DMA involves exciting a material with a periodic stress and monitoring the resultant strain for viscoelastic properties of the material with respect to temperature, humidity, vibration frequency, dynamic or static strain amplitude, or other parameter against time (162). The two primary uses are for determination of morphology including glass transitions and melts and checking polymer behavior at conditions simulating end use while maintaining temperature equilibrium. This method detects α- (first-order or glass) transitions, β- (side-chain motions) transitions, and γ- (crankshaft rotation of main-chain segments or single bond flips) transitions, and has about a 1000× greater sensitivity to DSC and about 100× greater sensitivity to modulated DSC for amorphous polymers. In this procedure, a specimen is placed under a fixed or free oscillatory stress and the strain with which the specimen responds is recorded. Polymers are typically

viscoelastic in nature, and have a dynamic response to the oscillatory stress controlled by the viscous component, which results in a strain that continues to increase until the stress is removed, but is not recoverable. The other component is the elastic response, which reacts instantaneously to the applied stress and is completely recovered when the stress is removed. Polymers respond with elements of each, resulting in a strain with the same frequency as the applied stress, but out of phase by an amount, δ, dependent on the relative elastic and viscous nature of the material (see Fig. 4) (163). Samples can be tested under different stress configurations, ie, tensile, flexural, compressive, and shear, by using a varying resonance frequency under a constant temperature or constant rate of temperature change. The tangent of δ is known as the loss factor and is the ratio of E'', the loss modulus, over E', the storage modulus; E is used for tensile (extensional deformation) whereas G is used for shear.

Stress levels are kept low within the elastic region of the material. Although solid-state testing is used most frequently, melt-state testing allows the examination of viscosity versus frequency at a set temperature and also shows the response of the shear storage and loss modulus (G' and G'') versus frequency. Solid-state testings of both amorphous and semicrystalline polymers by DMA have shown effects on tan δ values near the T_g for each type of material from differences in orientation by sample preparation method. For amorphous materials, the values of tan δ are higher in the temperature region slightly below the T_g as orientation increases in the sample; the same effect is seen for crystalline materials above the T_g (164). The interrelationship between temperature and frequency as well as time and frequency are well established (165). The equivalence of the effects of temperature and time in viscoelastic systems results in time–temperature superpositioning (166) and is related by the Williams–Landel–Ferry (WLF) equation (eq. 4) for amorphous polymers, where a_T is the shift factor, T is the measurement temperature, T_o is the reference temperature, and c_1 and c_2 are constants (167).

$$\log a_T = \frac{-c_1(T - T_0)}{c_2 + (T - T_0)} \tag{4}$$

This allows the production of master curves, which can be used to estimate changes in modulus or other properties over a long period of time by shorter tests over different temperatures. The Arrhenius relationship (eq. 5) for crystalline polymers or other transitions, where E_a is the activation energy and R the gas constant (8.3 J/mol), is as follows:

$$\text{Log } a_T = \frac{-E_a}{R(T - T_0)} \tag{5}$$

DMA of multiple frequency measurements over a range of temperatures allows the plotting of modulus versus time in similar master curves as generated by a series of short-term creep studies in a much shorter timeframe. There are potential problems with these predictions, such as internal stresses in amorphous polymers interfering in superpositioning loss modulus data near T_g (168), using data in temperature regions outside linear viscoelastic behavior

(169), or strains outside the linear regions. Studies on blends have been documented on styrene block copolymers with poly(α-methylstyrene) (170), unsaturated polyesters with elastomers (171), polyethylene copolymers with low ethylene content (172), and polycarbonate–poly(butylene terephthalate) (173). Furthermore, DMA is used to study the curing of thermoset systems (174–176). DMA has also been used to study the effects of additives of filled polymers (177,178) and the relaxation mechanisms of polycarbonate, metallocene polyethylene, and polypropylene fibers (179–181). The nonlinear behavior and deformation mechanisms of closed cell olefin foams were determined with DMA techniques (182). There are series of established standards for a variety of DMA techniques available from both ISO and ASTM as shown in the table below.

Recent developments have been in the area of microthermal analysis using thermal conductivity with thermal diffusivity signals or AFM to visualize specific areas or domains in the material and perform localized thermal analysis studies (183,184). Relaxational behavior over time and temperature is related to changes in free volume of the material. Positron annihilation lifetime spectroscopy (PALS) measurements of positron lifetimes and intensities are used to estimate both hole sizes and free volume within primarily amorphous phases of polymers. These data are used in measurement of thermal transitions (185,186) structural relaxation including molecular motions (187–189), and effects of additives (190), molecular weight variation (191), and degree of crystallinity (192). It has been used in combination with DSC to analyze the range of miscibility of polymethyl methacrylate poly(ethylene oxide) blends (193).

Another relatively recent development in thermal technique for polymers is equipment for reliable measurement of chemiluminescence. The luminescence is thought to be from the drop of an excited carbonyl group back to the neutral state after excitation from the termination of two peroxy radicals. Its use is primarily in determination of oxidation stability of polymers to determine an oxidative induction time (OIT) (194,195). It has also been used to monitor oxidation of polymers subjected to stress (196) and simulated weathering (197).

Another technique that is similar to DMA is dielectric thermal analysis which is covered under the Electrical Properties section.

Vicat softening temperature (ASTM D1525, ISO 306) uses a flat-ended needle penetration of 1 mm of the plastic specimen under controlled heating conditions to indicate short-term resistance to heat. For some plastics these curves can be extrapolated to zero force and zero rate of heat to give values in agreement with glass-transition data (198). Testing of deflection temperature under load (ASTM D648, ISO 75) determines bending resistance of plastic specimen under load and at a set rate of temperature increase. This test is highly influenced by the molded-in stresses and the thickness of the specimen tested. Annealing specimen to relieve stresses prior to testing improves reproducibility of the test but also results in higher values than unannealed specimen. Locati and co-workers have proposed monitoring of the complete deflection curve with both annealed and unannealed samples to obtain a $T_{0.25}$ that is a temperature characteristic of a material at zero stress (but dependent on deformation) and two stress sensitivity coefficients that are dependent on the thermomechanical history of the material to better indicate the material performance in applications (199).

Test area	Subject	ASTM	ISO
physical properties	specific gravity/density	D792, D1505	1183
	water absorption	D570	62
rheological properties	melt flow rate	D1238	1133
	capillary rheology	D3835	11443
	capillary rheology-screw	D5422	
	spiral flow-thermoset	D3132	
	solution viscosity	D2857	1628 1-5
mechanical properties	tensile	D638	527 1-4
	compressive	D695	604
	flexural	D790	178
	Charpy impact	D6110	179
	notched Izod impact	D256	180
	instrumented dart impact	D3763	6603-2
	Gardner/dart drop	D5420	6603-1
	tensile impact	D1822	8256
	Rockwell hardness	D785	2039-2
	creep	D2990	899
	fracture toughness	D5045, D5528, D6068	572
thermal properties	heat deflection temp.	D648	75 1-2
	Vicat softening temp.	D1525	306
	DSC	D5417	11357 1-3
	dynamic mechanical analysis	D5279, D4065, D5023, D5418, D5024, D5026, D4440, D4092	6721 1-10
optical properties	haze	D1003	14782
	transmittance	D1003	13648 1-2
	color	D2244, D6290, D7729	
electrical properties	dielectric strength	D149	IEC 243-1
	dielectric constant	D150	IEC 250
	volume/surface resistivity	D257	IEC 93
ignition properties	flammability	D635, D560, D3801, D3814, D1929, E176, UL94	871, 1210

	limited oxygen index	D2863	4589
	avg. extent of burning	D635	2782, 1210
environmental	chemical resistance	D543	175, 4600, 6252, 4599
	thermal aging	D5510	2578
	weathering	D1435, D4364, G26, D5071, D4674, G152, G153, D6360	4607, 877, 4665, 4892, 11507, 4892
	biodegradability	D5209, D5210, D5247, D5271, D5272, D5338, D5509, D5511, D5512, D5525, D5526, D5988, D6003	14851, 14852, 14853, 14855, 15985
	fungi	G21	846
	bacteria	G22	
	radiation	E1027	

5. Processing Properties

The flow properties of polymers, whether the viscosity of liquid thermosets prior to gelation or of molten thermoplastics, are important parameters for the proper processing of materials (see RHEOLOGY). Several test methods have been developed to predict or correlate to actual processing conditions or for quality control testing of polymers. For thermoplastics, the commonly used quality control method is melt flow rate (ASTM D1238 or ISO 1133). This technique can give values at melt index conditions that are inversely proportional to the molecular weight of homopolymers. However, the common addition of processing aids, lubricants, and fillers makes this correlation highly unreliable. Procedures that determine melt flow under two loads have been used primarily with polyolefins as an indication of molecular weight distribution. Melt flow rate values, although useful for quality control, are not indicative of the actual response of the material during processing, primarily due to the viscoelastic nature of polymers. Because polymers are non-Newtonian in flow, large differences in shear rate of the melt flow rate test ($1-50\ s^{-1}$) versus that of processing equipment, eg, extrusion ($10^2-10^3\ s^{-1}$) and injection molding ($10^3-10^5\ s^{-1}$), can cause large changes in the viscosity of most polymers.

Because processing conditions cover a wide range of shear rates, tests that can simulate both temperature and shear rate conditions are more useful in predicting flow properties. Several studies have been conducted on correlating common processing techniques that use torque rheometers, capillary rheometers, high pressure capillary rheometers, and oscillating disk rheometers for both thermoplastics and thermosets (202–204). Capillary rheometers have been designed to reach shear rates of $10^7\ s^{-1}$ and are used to study flow behavior at high shear (202). A typical set of curves of viscosity versus shear rate is shown in Figure 5 (205). A study of flow testing of ABS resins showed similar flow ranking of different grades of resin by using capillary rheology (ASTM D3835, ISO 14133), spiral flow molding, and on-machine rheometry (206,207), the last technique using an injection-molding machine as a rheometer. Capillary rheology tests using a screw rheometer in place of a piston have been published as ASTM D5422. Work is in development at ISO for determining extensional viscosity data as well as drawing properties using a rheometer for improved understanding of extrusion processing (208). Some work has been completed on using capillary rheology measurments on-line to measure rheological properties during polymerization (209).

Flow tests designed for thermosetting resins include a cup flow mold for flash-molding of powdered phenolic and alkyd materials (ASTM D731), spiral flow for low pressure thermosets (ASTM D3123), and torque rheometer techniques (ASTM D3795). In addition to these, tests for measuring time to gelation (gel) are important for processors to understand usage time and pot life (210). Dilute solution viscosity testing of polymers requires complete dissolution in the solvent without degradation or interaction with the solvent within the chosen temperature range of the tests. Data from these tests have been used to determine relative molecular weight of polymers (211).

New standard tests for determining pressure–volume–temperature (PVT) properties of materials using rheometers and other techniques (212,213) are being established to discover the correlation for the fundamental properties of plastics. These in combination with no-flow temperature, ejection temperature, and capillary rheology data are useful in predicting the behavior of molten plastic as it enters and fills a mold. Several mold-filling prediction computer programs are commercially available (214,215) to assist mold designers and plastic processors in developing plastic parts that have reduced stresses from the molding process, and in improving productivity with easier start-up of new molds and fewer rejected parts.

6. Mechanical Properties

Mechanical properties of plastics can be determined by short, single-point quality control tests and longer, generally multipoint or multiple condition procedures that relate to fundamental polymer properties. Single-point tests include tensile, compressive, flexural, shear, and impact properties of plastics; creep, heat aging, creep rupture, and environmental stress-cracking tests usually result in multipoint curves or tables for comparison of the original response to postexposure response.

Tensile properties are those of a plastic being pulled in an uniaxial direction until sufficient stress is applied to yield or break the material. Standard tests are ASTM D638 and ISO 527 parts 1–4. For many materials, Hooke's law is valid for a portion of the stress–strain curve. If stress is relieved during this portion of the testing, any strain that has occurred is fully recovered. Elastomers generally do not show a linear response nor a true yield point. Tensile curves can be used as an indication of polymer strength and toughness. Figure 6 shows the relationship normally seen for the stress necessary for yield or break with strength, whereas elongation beyond yield shows ductility (toughness). Similar curves can be generated for tests in comparison, flex, shear, and some forms of impact.

Mechanical properties are determined on solid polymers in arbitrary forms defined precisely by standard test methods in ISO, ASTM, or other national standards organizations. Parts are formed by either injection molding, compression molding, or milling from extruded sheet or molded plaques. Viscoelasticity of polymers dictates that the technique used to make the part must have a significant effect on the mechanical behavior of the polymer. For valid comparison of materials, they should be prepared similarly and conditioned under the same environment. Viscoelastic effects are also the reason for the rate of strain effects on the modulus values of materials under tensile, flexural, and compressive testing (216,217). The modulus of elasticity is also thickness-dependent, showing decreases as thickness increases in the plane-stress condition (0.1–2 mm) and the opposite effect at higher thicknesses where plane-strain conditions exist (218). Several types of impact testing have been developed to measure a plastic's response to a high rate of strain. Notched or Charpy Izod impact are pendulum impact tests essentially uniaxial in direction. Although both tests have been long established for quality control tests and material property data sheets, they are not useful in determining the impact response of a plastic in most applications.

ASTM D256 lists multiple cautions on using data from these tests. Notched Izod's primary practical value in characterizing a plastic material is to establish notch-sensitivity of the material. Drop-weight impacts, either manual or instrumented, give more practical information because of the multiaxial stresses found in these test procedures which are closer to normal impact events. Instrumented impact allows the recording of the full impact event as a stress–strain curve, showing similar characteristics to tensile or other modes of stress–strain tests. Instrumented impact is preferred for monitoring ductile–brittle transitions and determining the effects of polymer composition on material toughness. Analysis of DMA analysis and impact properties of various compositions of impact-modified polypropylene showed a direct correlation between the loss tangent of DMA tests and impact properties (219).

Creep, creep rupture, and stress relaxation tests are multiple-point tests requiring long periods of time (1000 h minimum) to generate useful data; these are standard tests for determining more fundamental polymer properties. Data for these tests are generated under several time–temperature–stress-level conditions in either tensile, flexural, compressive, or shear modes and combined into master curves using superpositioning theory (see AGING, PHYSICAL; VISCOELASTICITY). The low stress loads applied in creep tests, and thereby the low strain rates determined, require sensitive equipment for accurate measurements. Studies that normalize the stress required to produce a given strain in a given time to the stress producing that same strain after 24 h, have shown that plots of the normalized stress rates versus time over stress (24 h) give a single curve, which can be used with other short-term (days) creep tests at different stress levels to prepare master curves that can require up to 1 year for traditional data generation (220). Isometric curves can also be obtained similarly by using different temperatures for a given strain. Modulus values from these curves are used in plastic part design equations to predict part performance over the expected life of the part.

Fatigue testing of polymers may consist of static fatigue, ie creep rupture, or dynamic fatigue. Modes of cyclic fatigue include tension, compression, or shear, which use sinusoidal-, square-, and sawtooth-wave forms for applying stress, although varying strain can also be used in cyclic fatigue testing (see FATIGUE BEHAVIOR OF POLYMERS). Notching of specimen and high or low temperatures have been employed to accelerate the failure via embrittlement of the materials, but can lead to unwarranted extrapolation of the test data without additional tests (221).

Substantial work on the application of fracture mechanics techniques to plastics continues today (222–225) (see FRACTURE). The principle is based on failure stress proportionality to the square root of the energy required to create the new surfaces as a crack grows and inversely with the square root of the crack size originally determined with glasses. For the use of linear elastic fracture mechanics in plastics, certain assumptions must be met (226): (*1*) the material is linearly elastic; (*2*) the flaws within the material are sharp; and (*3*) plane strain conditions apply in the crack front region. The equation relating fracture toughness to modulus and energy release is given below for plane-stress and

plane-strain conditions :

$$\text{Plane-stress} \qquad K_c = (E\ G_c)^{1/2} = Y\sigma_f a^{1/2}$$

where K_c = fracture toughness, E = Young's modulus, G_c = critical energy release rate per unit crack length, σ_f = nominal applied stress at fracture, a = crack length (or 1/2; internal crack length), and Y = geometry factor.

$$\text{Plain-strain} \qquad K_c = (E/1 - v^2 G_c)^{1/2}$$

where ν = Poisson's ratio.

ASTM D5045 has been accepted for the determination of the critical stress intensity factor, *KIC*. Although *KIC* is temperature- and rate-dependent and the dependence is specific for any material, it is relatively independent of specimen geometry. Single-edge-notched beams are typically used for the test, but other geometries, eg, compact tension, short rod, and center-notched tension, have been used for the testing (227–231). Some plastics do not follow the mode outlined in D5045 at the thicknesses normally used in parts. These require the use of elastic plastic fracture mechanics using the *J*-integral parameter (232). More complex treatments of fracture incorporating nonlinear, viscoelastic effects have also been developed (233–235).

Hardness measurements such as Rockwell or Vicker's indentation properties are time-dependent as a result of the viscoelastic flow and relaxation processes (236) (see HARDNESS). Microhardness measurements have been used to correlate with other properties such as Young's modulus and compressive yield stress in polyethylenes (237) and glass-transition temperature of amorphous plastics (238). Scratch resistance in polyproplyene studies was found to have shear yielding as the main cause of plastic flow scratch pattern with tensile tear effects on the surface and shear-induced fracture on the subsurface (239).

7. Environmental Effects Tests

In practical applications of plastic materials, their mechanical properties can be significantly influenced by environmental factors of chemical exposure, temperature, radiation (photon and gamma ray), biological agents, and/or combinations of several of these factors at once. Few standard tests have been developed in these areas. Techniques and models used to extrapolate data from aging and environmental resistance tests on polymers have been proposed to predict service performance in various applications (240). This paper illustrates uses of Arrhenius, Avrami, WLF, and diffusion equations in evaluating exposure data and discusses their limitations. Mechanical properties can be determined by using ovens or cold-temperature chambers under the same procedures described in ASTM or ISO short-term tests to evaluate the effect of heat or cold. The length of exposure time, test conditions (at temperature or after being reconditioned to standard testing conditions after exposure), and reference material must all be stated to use these data. ISO 2578 addresses these variables, but allows the

tester to choose the characteristic for testing and the threshold value (limit of decline in performance). It recommends testing for 20,000 h and performing the test under standard room temperature conditions after heat exposure. ASTM is developing a standard for comparative indexing of heat-aged materials to original properties, but does not indicate a minimum exposure time. Thermal expansion testing also addresses the physical dimensional changes in plastic parts exposed to temperature changes. The change must be measured in each orthogonal direction, because polymers are not generally isotropic or homogeneous. ASTM D696 has been used for coefficient of linear thermal expansion. Shrinkage measurements are not related to low temperature measurements, but refer to the dimensions of post-molded parts compared to the mold dimensions or to post-molding shrinkage that involves short-term, high heat exposure with post-exposure dimensional measurements. Melting points of crystalline materials may be determined by capillary tube or hot-plate techniques, whereas softening point (ISO 306, ASTM D1525) by penetration or deflection under load (ISO 75, ASTM D648) is generally used for amorphous and semicrystalline polymers.

Chemical exposure of plastics may exhibit a wide range of effects with one chemical and one type of polymer, depending on the concentration of chemical agent, temperature of exposure, molded-in stresses within the specimen, applied stress level to the part during exposure, and formulation of the specific polymer grade. Standardized tests have been developed to evaluate the effects of chemical agents on plastics with and without external stress. Tests such as ASTM D543 and ISO 175 propose procedures for evaluating the effects of suggested chemicals on dimensions, appearance, and mass of the polymer specimen after the specimen has been immersed for a set period of time. Mechanical properties may also be checked if the specimen has maintained sufficient integrity to test. Tests in which stress is externally applied include both stress and strain techniques. ASTM D1693 uses bent strips of polyethylene with a cut, exposed to an aggressive surfactant and exposed until failure or 48 h. Several improvements have been suggested, primarily in better defining specimen preparation (241) or control of the amount of strain used (242). For blow-molded polyethylene bottles, accelerated test conditions of higher temperature and pressure were found applicable (243). Amorphous poly(ethylene terephthalate) used aqueous sodium hydroxide and creep crack growth rates to determine environmental stress-crack performance (244).

The method of caustics has also been used to study the formation of cracks and crazes formed by exposure of PMMA to solvents (245). ISO 4599 has been developed to better control the application of stress using a jig having the curve of the arc of a circle for shaping the specimen and maintaining a set curvature during exposure to the agent. After a predetermined time the specimen is tested for tensile or flexural properties and compared to preexposure test values. ISO 4600 uses the technique of impressing an oversized ball or pin into a hole drilled in the specimen to apply a strain.

Tests using a constant stress (constant load) normally by direct tension have been described in ISO 6252. This test takes the specimen to failure, or a minimum time without failure, and frequently has a flaw (drilled hole or notch) to act as a stress concentrator to target the area of failure. This type of testing, as well as the constant strain techniques, requires careful control of

specimen preparation and test conditions to achieve consistent results (246,247). Use of a slow strain rate with a four-point bend specimen configuration and constant load has been suggested as a method for ranking materials for environmental stress-crack resistance (248).

Weathering of plastic materials combines complex factors of temperature, radiation, oxidation, and moisture effects on a plastic part. Weathering effects vary with geography, time of year, and position of material being exposed. All of these effects make predicting the weatherability of a material extremely difficult. A recently completed study on the reproducibility of weathering data concluded that ranking of materials appears consistent although absolute data varies significantly from lab to lab (249). ISO 877 and ASTM G24 outline procedures for standardizing outdoor exposure of plastics under glass; ISO 4607 and ASTM D1435 are techniques for total exposure of plastic specimens to natural elements in racks and under specific climatic conditions. Frequently, only changes in physical appearance are measured after weathering; however, appropriate specimens can be exposed, mechanically tested, and compared to carefully stored control specimens (250). The long time periods required for outdoor weathering studies have led to the development of several accelerated techniques. The use of extreme and consistent climates, eg, South Florida or Arizona, and intensifying techniques for natural sunlight have been suggested to accelerate tests. ASTM D4364 has established a method for the use of a follow-the-sun rack with flat mirrors to reflect sunlight uniformly onto the test specimen as an intensifying technique. Because these techniques still require long exposure times to obtain results, in-lab acceleration tests to weather materials artificially have been developed. Various lamp sources have been used, such as low and high pressure mercury, carbon arc, and xenon arc. Although carbon arc lamps are still used to weather materials, xenon arc lamps are the preferred lamp for plastics weathering. These lamps simulate sunlight closely when appropriate filters are used (Fig. 7). Various correlations have been reported between xenon testing and outdoor weathering. For several plastics, 500 h in xenon arc testing, provided high humidity and water spray are used, are equivalent to 1 year of outdoor exposure. Some equipment manufacturers indicate that the ratio is one hour of accelerated to 10 h of outdoor exposure, whereas experimenters have found that the ratio can range from 1 h accelerated/5 h outdoor to 1 h accelerated/9 h outdoor when evaluated by the change in plastic color. Accelerated tests should be used to compare the relative performance of materials and ranking resistance to exposure, rather than for any direct correlation to outdoor weathering. Both ISO and ASTM have established practices for the use of carbon arc and xenon arc accelerated equipment. Recently, suggestions have been made for use of higher temperatures and irradiance levels to further accelerate weathering (251).

Fluorescent UV lamps within an apparatus that allows condensation cycles rather than the water spray typical of xenon arc tests have been developed for plastics testing. The spectral cutoff wavelength of the lamps used in the apparatus determines the severity of the test. Ultraviolet B (UVB) 313 lamps allow a significant irradiance component below 290 nm, which is normally filtered out by the earth's atmosphere. Ultraviolet A (UVA) 340 lamps have shown better correlation to the spectral irradiance of natural sunlight, although the visible light range is missing.

Other environmental testing standards have been developed for evaluating the effects of biological agents, either strains of fungi (ISO 846 or ASTM G21) or bacteria (ASTM G22), on mold growth on the plastic material, or if the plastic material has a toxic effect on the fungi. Longer-term outdoor exposure tests for resistance to microbial attack require geographic locations favorable to microbial growth or burial of the material in soil. ASTM E1027 is used for exposure of polymers to ionizing radiation. This can be used for testing the resistance to gamma rays, electrons, neutrons, etc. These tests are important for plastics used in the medical area to determine the resistance to sterilization techniques. A set of standards have been introduced at ASTM and ISO for the evaluation of biodegradable plastic materials. These standards have recommended standard conditions for a variety of environments to substantiate environmental performance of this new type of plastic material.

8. Optical Properties

Transparency, gloss, color, refractive index, and reflectance are the properties normally associated with aesthetics of plastic materials. In some areas, changes in optical properties, increases in haze after abrasion testing, color differences after weathering, and birefringence analysis of residual stress within a transparent part (252) are all used to measure the effects of applied stresses. Measurements of color, gloss, refractive index, and haze apply to many products beyond plastics and use similar techniques. Reference should be made to this general topic for detailed information.

One of the most widely accepted measurements of color in plastics is based on standards developed by the Commission Internationale de l'Eclairage (CIE) for illuminants and observers to establish tristimulus values. A common color scale used to describe color in numeric terms of lightness and hue is the L-a-b tristimulus system, where L is scaled vertically from a perfect white with a value of 100 to a perfect black at 0; a is positive for red and negative for green; and b is positive for yellow and negative for blue. Spectrophotometers are used to measure the full reflectance of a colored material over the visible range and convert to the tristimulus values via microprocessors. Color as viewed under various CIE illuminants and/or observers can be determined by a single spectrophotometric analysis as the microprocessor computes the tristimulus values for each set of conditions. Color-matching of an object can be completed by comparing spectral curves generated through the use of the spectrophotometer. However, many factors, such as gloss, texture, opacity, and changes in illuminant and observer, complicate the visual appearance of a color with the spectral curve of a color. ASTM D1729 establishes procedures for visual evaluation of color and defines illuminant, viewing conditions, and use of standards for comparison; ASTM D2244 describes instrumental color evaluation techniques. Specular gloss, the relative reflectance of a specimen in the specular direction, is usually measured at 60° angle of incidence for most plastics. High gloss materials may be measured at 20° incidence and low gloss specimens at 85° incidence using ASTM D523. For films, ASTM D2457 uses measurements at 20°, 60°, and 45° angles of incidence.

9. Electrical Properties

Dielectric analysis (DEA) or dielectric thermal analysis (DETA) is similar to DMA (see Dielectric Relaxation). In DEA, the movement of dipoles or other ionic species that can be electrically stimulated allows the monitoring of changes in ionic conductivity. Similar to DMA phase angle δ, in DEA this is related to the lag of the polarization induced in an insulator placed in an alternating electrical field. The energy dissipated as heat is proportional to the dielectric loss ε'', and the energy stored is the real part of the dielectric constant, ε'. The electrical technique is considered more sensitive to transitions below T_g than DMA (253). It is also more sensitive to β-transitions frequently linked to impact strength and long-term mechanical strength (254). Dielectric analysis has a broader and higher range of frequencies than DMA. Changes in permittivity with time in DEA measurements have been correlated with moisture content change in polymers (255) and have become an on-line technique for monitoring moisture in polymers. Thermally stimulated conductivity (TSC) uses the technique of polarizing a polymer at different temperatures, quenching the sample, and measuring the depolarizing current as the material is heated at a controlled rate (256). The rate of repolarization is related to the relaxation times of internal motions. When DEA was used to characterize the alpha relaxation process of an interphase formation in composite material, the process was found to be diffusional rather than a resin curing process (257). A combination of DMA and DEA in a study on the effects of low molecular weight additives in poly(ethylene terephthalate) was able to resolve that beta peak had two different relaxation processes correlating with different molecular motions in the polymer chain (258). DMA relaxation spectroscopy was also used to relate the structure of lateral groups of aromatic polyamides to molecular mobility (259). Inverse gas chromatography has been used to predict and measure diffusion coefficients using a method at finite concentration of solvent (260). It has also been used to examine surface properties of solid materials (261).

Excellent insulating properties, along with the ability to be structural components, make plastics the ideal candidate materials for electrical applications. Although generally used as insulators, carbon black or carbon fiber can be added to make plastic materials electrically conductive, thereby expanding their usefulness in the electronics area.

Standard testing of electrical properties of plastics includes dielectric strength, permittivity, dissipation factor, surface and volume resistivity, and arc resistance. Dielectric strength is the maximum voltage required for breakdown and is determined by one of three techniques: short-time, slow-rate or slow-rise, and step-by-step. The two last techniques use data from the short-time test to determine a starting point. Dielectric strength is thickness-dependent with thin foils being used in specific space-saving devices.

Permittivity gives an indication of the electrical storage ability of a conductor (behaving as a capacitor). The thinner the material, the higher the permittivity or capacitance, allowing use of plastic foils in areas where high capacitance is required. However, when plastics are used as insulators, low permittivity is required. Resistivity testing can be either volume, relating to leakage

of current through the body of the insulator, or surface, relating to a surface layer of moisture or contaminant leading to electrical loss.

Arc resistance or tracking resistance is the resistance of a material to a high voltage arc or discharge. ASTM has published three methods to test this phenomenon, depending on the conditions to be tested: D495 for high voltage, low current, dry arc resistance; D2132 for dust and fog tracking; and D2302 for liquid-contaminant inclined-plane tracking. A comparative tracking index (CTI) technique uses a low frequency, low level current applied between electrodes while allowing drops of aqueous solution to fall between electrodes at 30-s intervals. This technique is described in ASTM D3638. However, the results or values obtained from these tests cannot be used in design studies (262).

Electromagnetic interference (EMI) testing has become more prevalent for materials that either emit or are affected by EMI. Shielding efficiency (SE) of materials is determined by measuring electric field strength between a transmitter and receiver with or without the presence of the material under test.

Underwriters' Laboratories (UL) is an independent, nonprofit organization that develops standards for safety in electrical products. UL 746 A, B, and C describe tests and limits for materials used in electrical equipment; UL 746 D lists test requirements for the fabricated plastic parts (263).

10. Flammability Properties

Plastics have become an important material in the construction industry and are used in areas of insulation, wire coating, flooring materials, and piping; they are also considered for structural components as foam panels and plastic wood. As use in the industry has grown, so has concern about the fire properties of these materials. Tests to determine ignition resistance, flame spread, heat release, and smoke or toxic gas release have been developed. However, the results of these tests are not applicable to the performance of the materials under actual fire conditions. These small-scale tests are intended for quality control and potential hazard ranking. Several organizations that go beyond testing standard bodies such as ASTM or the International Electrotechnical Commission (IEC) have developed tests and/or regulations for the use of plastics in electrical appliances or buildings. A listing of some of these tests is given in ASTM D3814. General fire test terminology is given in ASTM E176. Ignition temperature tests ISO 871 and ASTM D1929 have procedures using small external pilot flames. The limiting oxygen index test has been used in quality control primarily for its good reproducibility, but cannot be used to predict fire performance. ISO 4589 and ASTM D2863 determine the minimum oxygen concentration required to support flaming combustion under set conditions.

UL 94 flame testing of plastics is similar to ASTM D635 for horizontal burn and ASTM D568 and D3801 for vertical burn. UL lists both materials and fabricated products meeting the various 94 requirements in a publication (264). Rate of heat release data are highly important in determining fire behavior, but few tests have been established. Equipment proposed by Factory Mutual has been used in fundamental fire modeling studies (265). The cone calorimeter as described by the National Institute of Standards Technology (NIST) utilizes both

vertical and horizontal specimens (266). Refinements of this equipment have allowed testing in the reduced oxygen atmosphere typically found under fire conditions (267). Smoke generation tests have used changes in light absorption of a photoelectric cell within a confined chamber as the primary measurement. Results are reported as percent obscuration or smoke density. Flame or radiant panels can be used as the ignition source in these tests.

11. Nondestructive Testing

Nondestructive testing of materials is defined as any test that does not damage the plastic piece beyond its intended use. These can be visual and, in some cases, mechanical tests. However, the term is normally used to describe X-ray, nuclear source, ultrasonics, atomic emission, as well as some optical and IR techniques for polymers. Nondestructive testing is used to determine cracks, voids, inclusions, delamination, contamination, lack of cure, anisotropy, residual stresses, and defective bonds or welds in materials.

X-ray techniques can readily determine voids down to 1 mm in diameter and cracks (as long as the plane of the crack is close to the direction of the ray) (268). Nuclear sources and gamma and beta rays have been used to measure the thickness of extruded plastic sheet. For ultrasonics, the frequency used for plastics ranges between 0.5 and 5 MHz. However, isolated defects smaller than a wavelength are difficult to detect with this technique. Ultrasonics have also been used to determine elastic modulus, shear modulus, and Poisson's ratio via the relationship of sound wave velocities through a material (268,269). In studies with blends, the variation of the ultrasonic velocity with composition of a blend is nonlinear where the blend shows incompatibility and linear where it is compatible (270). Holographic interferometry uses an expanded beam of light from a laser source divided by a beam splitter, with one portion hitting the object and the other hitting a recording screen. When both beams are combined at the screen a unique interference pattern is formed. Comparison of this generated image with another of the object under stress produces a fringe pattern for analysis. The maximum depth/diameter ratio for a detectable defect is less than 0.2 (271).

Thermal imaging is sensitive to IR radiation that detects temperature changes over the surface of a part when heat has been applied. Thermal diffusion in a solid is affected by variation in composition or by the presence of cracks, voids, delaminations, etc; the effects are detected by surface temperature changes. Defects cannot be detected if their depth below the surface is more than two to three times their diameter. Nondestructive testing has been primarily used for composites and analysis of adhesive bonds or welds. Several studies are documented in the literature (272–274).

12. Other Tests

A variety of methods have been used to evaluate diffusion or permeability of gases and solvents with polymers: FTIR spectra of CO_2 allowed the determination of apparent diffusion coefficients of the gas in membranes of rubbery and

glassy polymers from desorption kinetics (275); internal reflection FTIR was used to monitor water uptake by a polymer film (276); spin probe techniques have been used in the study of high permeability and high free volume glassy polymers (277); and an *in situ* gravimetric method using an electro-balance was used to determine solubility and diffusivity of gases in polymers over a range of temperatures and pressures (278).

There are other tests for polymers that are not included in this review including some density, filler analysis techniques and other physical tests. For convenience, a listing of ASTM and ISO standards for the major test in this work is provided in the references.

BIBLIOGRAPHY

"Plastics Testing" in *ECT* 2nd ed., Vol. 15, pp. 811–831, by E. Horowitz, National Bureau of Standards; in *ECT* 3rd ed., Vol. 18, pp. 207–228, by E. Horowitz, The Johns Hopkins University; in *ECT* 4th ed., Vol. 19, pp. 316–347, by Barbara J. Furches, The Dow Chemical Company; "Plastics Testing" in *ECT* (online), posting date: December 4, 2000, by Barbara J. Furches, The Dow Chemical Company.

CITED PUBLICATIONS

1. J. M. Chalmers and co-workers, *Analyst* **123**, 579–586 (1998).
2. P. C. Painter, M. M. Coleman, and J. L. Koenig, *Theory of Vibrational Spectroscopy with Application to Polymers*, John Wiley & Sons, Inc., New York, 1981.
3. G. Bucci and T. Simonazzi, *J. Polym. Sci. Part C-7* 203 (1964).
4. A. Rjeb and co-workers, *J. Appl. Polym. Sci.* **77**, 1742–1748 (2000).
5. P. Musto and co-workers, *J. Polym. Sci. Part B* **35**, 1055–1066 (1997).
6. M. J. Elwell and A. J. Ryan, *Polymer* **37**, 1353–1361 (1996).
7. J. M. Garcia-Martinez and co-workers, *J. Appl. Polym. Sci.* **73**, 2837–2847 (1999).
8. T. R. Crompton, *The Analysis of Plastics*, Elsevier Science, Inc., Elmsford, N.Y., 1986.
9. D. Battiste and co-workers, *Anal. Chem.* **53**, 2232 (1981).
10. P. J. DesLauriers and co-workers, *Polymer* **43**(1), 159–170 (2002).
11. D. O. Hummel and F. Scholl, *Atlas of Polymers and Plastics Analysis*, 2nd ed., Vol. **1**, Carl Hanover Verlag, Munich, 1978.
12. C. D. Craver, *Infra-Red Spectra of Plasticizers and Other Additives*, 2nd ed., The Coblentz Society, Kirkwood, Mo., 1980.
13. Y. Wang and co-workers, *J. Polym. Sci. Part B* **36**, 783–788 (1998).
14. B. R. Kiland and co-workers, *Polymer* **41**, 1597–1606 (2000).
15. E. E. C. Monteiro and J. Fonseca, *Polym. Test.* **18**, 281–286 (1999).
16. A. C. Middleton and co-workers, *J. Appl. Polym. Sci.* **79**, 1825–1837 (2001).
17. A. Kaito and K. Nakayama, *Macromolecules* **25**, 4882 (1992).
18. J. A. Jansen and co-workers, *Polymer* **35**, 2970 (1994).
19. M. Clayborn and co-workers, *J. Appl. Spectrosc.* **45**, 279 (1991).
20. J. M. Chalmers and co-workers, *Spectrosc. Int. J.* **8**, 13 (1990).
21. J. M. Chalmers and co-workers, *Micron* **27**, 315 (1996).
22. T. Rohe and co-workers, *Talanta* **50**, 283–290 (1999).
23. M. G. Hansen and S. Vedula, *J. Appl. Polym. Sci.* **68**, 859–872 (1998).

24. M. Shenton and co-workers, *Polym. Int.* **49**, 1007–1013 (2000).
25. M. G. Hansen, *SPE ANTEC* **37**, 840 (1991).
26. G. C. Pandey, *Analyst* **112**, 231–232 (1989).
27. F. Eng and C. Shebih, *SPE ANTEC* **35**, 1174 (1989).
28. D. Battiste and co-workers, *Anal. Chem.* **53**, 73 (1981).
29. D. Mathieu and A. Grand, *Polymer* **39**, 5011–5017 (1998).
30. J. P. Tomba and co-workers, *J. Polym. Sci. Part B* **38**, 1013–1023 (2000).
31. T. Sundell and H. Fagerholm, *Polymer* **37**, 3227–3231 (1996).
32. Y. Ward and Y. Mi, *Polymer* **40**, 2465–2468 (1999).
33. R. L. Morgan and co-workers, *Polymer* **42**, 2121–2135 (2001).
34. M. Van and co-workers, *J. Appl. Polym. Sci.* **79**, 426–436 (2001).
35. K. Kober and co-workers, *J. Polym. Sci. Part B* **36**, 2829–2833 (1998).
36. H. Buijs and co-workers, *Am. Lab.* **21**(2), 62–69 (1989).
37. E. Da Silva and M. Tavares, *J. Appl. Sci.* **67**, 449–453 (1999).
38. L. Mendes and co-workers, *Polym. Test.* **15**(1), 53–68 (1996).
39. M. Tavares and L. Mendes, *Polym. Test.* **19**, 399–404 (2000).
40. R. Wu and co-workers, *Polymer* **43**(1), 171–176 (2002).
41. A. Striegel and M. Krejsa, *J. Polym. Sci. Part B* **38**, 3120–3135 (2000).
42. M. Tavares and C. Mothe, *Polym. Test.* **17**, 289–295 (1998).
43. A. Maxwell and co-workers, *Polymer* **39**, 6835–6849 (1998).
44. K. Plochokca and H. Harwood, *ACS Div. Polym. Chem. Pap.* **19**, 240 (1978).
45. I. Pesneau and co-workers, *J. Appl. Sci.* **79**, 1556–1562 (2001).
46. W. Weglarz and co-workers, *J. Polym. Sci. Part B* **38**, 2487–2506 (2000).
47. C. Choi and co-workers, *J. Polym. Sci. Part B* **35**, 2551–2558 (1997).
48. M. Tavares, *Polym. Test.* **19**, 899–904 (2000).
49. S. Lehmann and co-workers, *J. Polym. Sci. Part B* **36**, 693–703 (1998).
50. H. Pasch and K. Rode, *Polymer* **39**, 6377–6383 (1998).
51. U. Fuchslueger and co-workers, *J. Appl. Polym. Sci.* **72**, 913–925 (1999).
52. M. Janco and co-workers, *J. Polym. Sci. Part A* **38**, 2767–2778 (2000).
53. M. Riess and R. van Eldik, *J. Chrom. A* **827**(1), 65–71 (1998).
54. J. C. J. Bart, *Polym. Test.* **20**, 729–740 (2001).
55. F. C.-Y. Wang, *J. Chrom. A* **843**, 413–423 (1999).
56. M. Minagawa and co-workers, *J. Appl. Polym. Sci.* **79**, 473–478 (2001).
57. F. C.-Y. Wang and D. Meunier, *J. Chrom. A.* **888**, 209–217 (2000).
58. R. Lehrle and co-workers, *Polym. Degrad. Stab.* **67**(1), 21–33 (2000).
59. H. Ohtani and co-workers, *Macromolecules* **17**, 465 (1984).
60. F. C. Wang and P. B. Smith, *Anal. Chem.* **68**, 3033 (1996).
61. R. Yang and co-workers, *J. Appl. Polym. Sci.* **81**, 359–363 (2001).
62. D. Weber, *Int. Lab.* **21**, 51 (1991).
63. T. Wampler, *J. Chrom. A* **842**, 207–220 (1999).
64. F. C. Wang, *Anal. Chem.* **71**, 2037 (1999).
65. F. C. Wang, *J. Chrom. A.* **886**, 225–235 (2000).
66. F. C. Wang, *J. Chrom. A.* **883**, 199–210 (2000).
67. F. C. Wang and W. Buzanowski, *J. Chrom. A.* **891**, 313–324 (2000).
68. F. C. Wang, *J. Chrom. A.* **891**, 325–336 (2000).
69. M. A. Robeson and co-workers, *J. Chromatogr.* **505**, 375 (1990).
70. T. Meyer-Dulheuer, *Shimadzu Seminar*, Duisburg, 1998.
71. J. C. J. Bart, *Polym. Test.* **20**, 729–740 (2001).
72. A. R. Berens and co-workers, *J. Appl. Polym. Sci.* **19**, 3169–3172 (1975).
73. S. W. Bigger and co-workers, *Preprints 37th International Symposium on Macromolecules*, Gold Coast, 1998, p. 377.
74. B. L. Zimmering and co-workers, *J. Appl. Polym. Sci.* **69**, 1875–1883 (1998).

75. M. J. Carrott and co-workers, *Analyst* **123**, 1827–1833 (1998).
76. J. Hay and co-workers, *Polym. Commun.* **26**(6), 175 (1984).
77. D. Rueda and co-workers, *Calliga. Polym. Lett.* **29**, 9, 258 (1983).
78. N. T. Wakelyn, *J. Polym. Sci., Polym. Lett.* **25**, 25 (1987).
79. B. Goderis and co-workers, *J. Polym. Sci. Part B* **37**, 1715–1738 (1999).
80. G. Bodor and co-workers, *J. Polym. Sci. Part B* **34**, 485–496 (1998).
81. P. Cebe, L. Lowry, and S. Chung, *SPE ANTEC* **35**, 1120 (1989).
82. O. Krathy, in O. Glatter and O. Krathy, eds., *Small-Angle X-Ray Scattering*, Academic Press, Inc., New York, 1982.
83. J. Barnes and F. Mopsik, *SPE ANTEC* **34**, 1178 (1988).
84. R. Xie, B. Yang, and B. Jiang, *J. Polym. Sci. Part B* **34**, 1489–1499 (1996).
85. I. Campoy, M. Gomez, and C. Marco, *Polymer* **41**, 2295–2299 (2000).
86. C.-I. Huang and J.-R. Chen, *J. Polym. Sci. Part B* **39**, 2705–2715 (2001).
87. M. Song and co-workers, *J. Appl. Polym. Sci.* **79**, 1958–1964 (2001).
88. M. Ishaq, J. Blackwell, and S. Chvalun, *Polymer* **37**, 477–483 (1996).
89. A. Kawaguchi and co-workers, *J. Polym. Sci. Part B* **38**, 838–845 (2000).
90. M. A. Jones, T. P. Russell, and D. Y. Yoon, *Proceedings of Polymer Material Science & Engineering*, San Diego, Calif., 1993, p. 394.
91. P. G. deGennes, *Scaling Concepts in Polymer Physics*, Cornell University Press, Ithaca, New York, 1979.
92. M. A. Jones, T. P. Russell, and D. Y. Yoon, *Proceedings of Polymer Material Science & Engineering*, San Diego, Calif., 1993, p. 396.
93. J. Maugey, T. Van Nuland, and P. Navard, *Polymer* **42**, 4353–4366 (2001).
94. K. Wallheinke and co-workers, *Polym. Test.* **17**, 247–255 (1998).
95. K. Swaminathan and D. Marr, *J. Appl. Polym. Sci.* **78**, 452–457 (2000).
96. D. Raghavan and co-workers, *J. Polym. Sci. Part B* **39**, 1460–1470 (2001).
97. S. Gould and co-workers, *J. Appl. Polym. Sci.* **74**, 2243–2254 (1999).
98. M. Zhang and co-workers, *J. Appl. Polym. Sci.* **80**, 2218–2227 (2001).
99. J. Feng and co-workers, *Polymer* **42**, 2259–2262 (2001).
100. G. Merle and co-workers, *Polym. Test.* **18**, 217–229 (1999).
101. F. Oulevey and co-workers, *Polymer* **41**, 3087–3092 (2000).
102. H. Oyama, T. Solberg, and J. Wightman, *Polymer* **40**, 3001–3011 (1999).
103. Z. Veksli, M. Andreis, and B. Rakvin, *Prog. Polym. Sci.* **25**, 949–986 (2000).
104. Z. Veksli, M. Andreis, and D. Campbell, *Polymer* **39**, 2083–2088 (1998).
105. G. Muller, R. Stadler, and S. Schlick, *Makromol. Chem. Rapid Commun.* **13**(2), 117–124 (1992).
106. G. G. Cameron and co-workers, *Eur. Polym J.* **27**, 1181–1186 (1991).
107. H. Tenhu and K. Voahtera, *Eur. Polym. J.* **27**, 717–722 (1991).
108. W. P. Chen and S. Schlick, *Polymer* **31**, 308–314 (1990).
109. S. Commereuc and co-workers, *J. Appl. Polym. Sci.* **69**, 1107–1114 (1998).
110. T. Dumelow, S. R. Holding, and L. J. Maisey, *Polymer* **24**, 307 (1983).
111. W. C. Taylor and L. H. Tung, Paper presented at *140th Meeting of the American Chemical Society*, Chicago, Ill., 1961.
112. R. Russ, K. Guo, and L. Delong, *SPE ANTEC* **34**, 983 (1988).
113. V. Shah, *Handbook of Plastics Testing Technology*, John Wiley & Sons, Inc., New York, 1984, p. 179.
114. J. Choi, *SPE ANTEC* **34**, 1013 (1988).
115. J. M. Guenet and co-workers, *J. Appl. Polym. Sci.* **21**, 2181 (1977).
116. S. Mori, *Anal. Chem.* **61**, 1321–1325 (1989).
117. J. Sebastian and R. Register, *J. Appl. Polym. Sci.* **82**, 2056–2069 (2001).
118. J. L. Viony and J. Lesec, in A. Abe, ed., *Advances in Polymer Science*, Springer-Verlag, Berlin, 1994.

119. L. Verdurmen-Noel, L. Baldo, and S. Bremmers, *Polymer* **42**, 5523–5529 (2001).
120. M. Montaudo, *Polymer* **43**, 1587–1597 (2002).
121. S. Podzimek and T. Vlcek, *J. Appl. Polym. Sci.* **82**, 454–460 (2001).
122. S. Podzimek, T. Vlcek, and C. Johann, *J. Appl. Polym. Sci.* **81**, 1588–1594 (2001).
123. L. Wold and co-workers, *J. Polym. Sci., Polym. Phys.* **20**, 441 (1982).
124. L. Britto and co-workers, *J. Polym. Sci. Part B* **37**, 539–552 (1999).
125. B. Gabriel and D. Lilge, *Polymer* **42**, 297–303 (2001).
126. J. Soares, R. Abbott, and J. Kim, *J. Polym. Sci. Part B* **38**, 1267–1275 (2000).
127. A. R. McGhie, in R. G. Linford, ed., *Thermal Analysis Techniques in Electrochemical Science and Technology of Polymers-2*, Elsevier Publishing Co., Inc., New York, 1990, p. 202.
128. J. Chiu, *Appl. Polym. Symp.* **2**, 25 (1966).
129. L. H. Perng, *J. Polym. Sci. Part A* **38**, 583–593 (2000).
130. P. Moulinie and co-workers, *Polym. Test.* **15**(1), 75–89 (1996).
131. C. A. Wilkie, *Polym. Degrad. Stab.* **66**, 301–306 (1999).
132. L. H. Perng, *J. Appl. Polym. Sci.* **79**, 1151–1161 (2001).
133. J. J. Maurer, in E. Turi, ed., *Thermal Characterization of Polymeric Materials*, Academic Press, Inc., New York, 1981, p. 585.
134. H. E. Bair, in E. Turi, ed., *Thermal Characterization of Polymeric Materials*, Academic Press, Inc., New York, 1981, p. 845.
135. M. P. Sepe, in N. P. Cheremisinoff, ed., *Elastomer Technology Handbook*, CRC Press, Inc., Boca Raton, Fla., 1993, p. 139.
136. M. P. Sepe, in N. P. Cheremisinoff, ed., *Elastomer Technology Handbook*, CRC Press, Inc., Boca Raton, Fla., 1993, p. 148.
137. Rosa and co-workers, *Polym. Test.* **19**, 523–531 (2000).
138. J. Rodriguez-Cabello and co-workers, *J. Appl. Polym. Sci.* **60**, 1709–1717 (1996).
139. R. Phillips and J. A. Manson, *J. Polym. Sci. Part B* **35**, 875–888 (1997).
140. K. Jokela and co-workers, *J. Polym. Sci. Part B* **39**, 1860–1875 (2001).
141. J. L. Vilas and co-workers, *J. Appl. Polym. Sci.* **79**, 447–457 (2001).
142. S. Li, E. Vuorimaa and H. Lemmetyinen, *J. Appl. Polym. Sci.* **81**, 1474–1480 (2001).
143. K. de la Caba and co-workers, *Polym. Int.* **45**, 333–338 (1998).
144. J. H. Hou and J. M. Bai, *SPE ANTEC* **33**, 946 (1987).
145. B. Wunderlich, in E. Turi, ed., *Thermal Characterization of Polymeric Materials*, Academic Press, Inc., New York, 1981, Chapts. 2 and 3.
146. P. Soni, *SPE Seminars*, Chicago, Ill., June, 1991.
147. L. C. E. Struik, *Physical Aging in Amorphous Polymers and Other Materials*, Elsevier, Amsterdam, the Netherlands, 1978.
148. J. J. Maurer, in E. Turi, ed., *Thermal Characterization of Polymeric Materials*, Academic Press, Inc., New York, 1981, Chapt. 6.
149. S. W. Shalaby and H. E. Bair, in E. Turi, ed., *Thermal Characterization of Polymeric Materials*, Academic Press, Inc., New York, 1981, Chapt. 4.
150. H. E. Bair, *Polym. Eng. Sci.* **14**, 202 (1974).
151. M. Song, A. Hammiche, and H. Pollock, *Polymer* **37**, 5661–5665 (1996).
152. A. Vatalis and co-workers, *Thermochem. Acta* **372**(1/2), 33–38 (2001).
153. T. G. Fox, *Bull. Am. Phys. Soc.* **1**(2), 123 (1956).
154. M. Gordon and J. S. Taylor, *J. Appl. Chem.* **2**, 493 (1952).
155. P. R. Couchman, *Macromolecules* **11**, 1156 (1978).
156. J. Janimak and G. Stevens, *Thermochim. Acta* **332**(2), 125–142 (1999).
157. M. Song, *J. Appl. Polym. Sci.* **81**, 2779–2785 (2001).
158. I. Okazaki and B. Wunderlich, *J. Polym. Sci. Part B* **34**, 2941–2952 (1996).
159. M. P. Sepe, in N. P. Cheremisinoff, ed., *Elastomer Technology Handbook*, CRC Press, Inc., Boca Raton, Fla., 1993, p. 157.

160. M. P. Sepe, in N. P. Cheremisinoff, ed., *Elastomer Technology Handbook*, CRC Press, Inc., Boca Raton, Fla., 1993, p. 165.
161. R. W. Thomas and M. W. Cadwallader, Technical data, TA Instruments Hotline, Wilmington, Del., June, 1990.
162. J. Gearing, in R. Brown, ed., *Handbook of Polymer Testing*, Marcel Dekker, Inc., New York, 1999, p. 501.
163. A. R. McGhie, in R. Linford, ed., *Electrochemical Science and Technology of Polymers-2*, Elsevier Applied Science Publishers, Ltd., London, 1990, p. 218.
164. C. Rohm and P. Herh, *SPE ANTEC* **34**, 1135 (1988).
165. J. D. Ferry, *Viscoelastic Properties of Polymers*, 3rd ed., John Wiley & Sons, Inc., New York, 1980.
166. L. H. Sperling, *Introduction to Physical Polymer Science*, John Wiley & Sons, Inc., New York, 1986, p. 384.
167. A. R. McGhie, in R. Linford, ed., *Electrochemical Science and Technology of Polymers-2*, Elsevier Applied Science Publishers, Ltd., London, 1990, p. 266.
168. C. L. Rohn, *SPE ANTEC* **35**, 870 (1989).
169. A. R. McGhie, in R. Linford, ed., *Electrochemical Science and Technology of Polymers-2*, Elsevier Applied Science Publishers, Ltd., London, 1990, p. 204.
170. C. D. Han and co-workers, *Macromolecules* **22**, 3443–3451 (1989).
171. J. Sahai, K. Nakamura, and S. Inoue, *SPE ANTEC* **36**, 1912 (1990).
172. M. P. Sepe, in N. P. Cheremisinoff, ed., *Elastomer Technology Handbook*, CRC Press, Inc., Boca Raton, Fla., 1993, p. 220.
173. Y. Feng, X. Jin, and J. Hay, *J. Appl. Polym. Sci.* **68**, 395–401 (1998).
174. S. Simon, G. Mckenna, and O. Sindt, *J. Appl. Polym. Sci.* **76**, 495–508. (2000).
175. S. Markovic and co-workers, *J. Appl. Polym. Sci.* **81**, 1902–1913 (2001).
176. J. Hiltz, S. Kuzak, and P. Waitkus, *J. Appl. Polym. Sci.* **79**(3), 385–395 (2001).
177. K. Lozano and E. Barrera, *J. Appl. Polym. Sci.* **79**(1), 125–133 (2001).
178. S. Diez-Gutierrez and co-workers, *Polymer* **40**(19), 5345–5353 (1999).
179. M. D. Shelby and co-workers, *J. Polym. Sci. Part B* **39**(1), 32–46 (2001).
180. K.-H. Nitta and A. Tanaka, *Polymer* **43**, 1219–1226 (2001).
181. O. Fri cova and co-workers, *Acta Polym.* **49**, 495–501 (1998).
182. M. Rodriguez-Perez and J. de Saja, *Polym. Test.* **19**, 831–848 (2000).
183. W. Xie and co-workers, *Thermochem. Acta* **367–368**, 135/142 (2001).
184. M. Song and co-workers, *J. Appl. Polym. Sci.* **81**, 2136–2141 (2001).
185. A. Uedono and co-workers, *J. Polym. Sci. Part B* **36**, 1919–1925 (1998).
186. P. Ramachandra and co-workers, *Polymer* **37**, 3233–3239 (1996).
187. T.-T. Hsieh, C. Tiu, and G. Simon, *J. Appl. Polym. Sci.* **82**, 2252–2267 (2001).
188. W. J. Davis and R. A. Pethrick, *Polym. Int.* **45**, 395–402 (1998).
189. H. Higuchi, A. Jamieson, and R. Simha, *J. Polym. Sci. Part B* **34**, 1423–1426 (1996).
190. J. Borek and W. Osoba, *J. Polym. Sci. Part B* **34**, 1903–1906 (1996).
191. H. Mohamed and N. Abd El-Aziz, *Polymer* **42**, 8013–8017 (2001).
192. G. Dlubek and co-workers, *J. Polym. Sci. Part B* **40**(1), 65–81 (2002).
193. J. C. Machado and co-workers, *J. Polym. Sci. Part B* **38**, 1045–1052 (2000).
194. P. K. Fearon and co-workers, *J. Appl. Polym. Sci.* **79**, 1986–1993 (2001).
195. G. Ablblad and co-workers, *Polym. Test.* **16**(1), 59–73 (1997).
196. K. Jacobson and co-workers, *Polym. Test.* **18**, 523–531 (1999).
197. D. Kockott, *Polym. Test.* **20**, 725–727 (2001).
198. D. Crofts, RAPRA Research Report, No. 200, Rubber and Plastics Research Association, Shrewsburg, U.K., 1972.
199. G. Locati, S. Poggio, and J. Rathenow, *Polym. Test.* **16**, 363–377 (1997).
200. J. A. Brydson, *Flow Properties of Polymer Melts*, 2nd ed., Godwin/Plastics and Rubber Institute, 1981.

201. H. Takahashi, T. Matsuoka, and T. Kurauchi, *J. Appl. Polym. Sci.* **30**, 4669 (1985).
202. Dow Chemical Company, Technical data, Midland, Mich., 1993.
203. M. A. Couch and D. M. Binding, *Polymer* **41**, 6323–6334 (2000).
204. N. Sombatsompop and N.-T. Intawong, *Polym. Test.* **20**(1), 97–103 (2000).
205. J.-Z. Liang, *Polym. Test.* **20**(1), 29–31 (2000).
206. K. T. Paul, *RAPRA Bulletin*, Rubber and Plastics Research Association, Shrewsburg, U.K., Feb. 1972.
207. B. J. Furches and G. Kachin, *SPE ANTEC* **35**, 1663 (1989).
208. R. J. Groleau, *SPE ANTEC* **35**, 1183 (1989).
209. J. Covas, J. Nobrega, and J. Maia, *Polym. Test.* **19**(2), 165–176 (2000).
210. P. Starch and P. Kantla, *Kem-Kemi* **3**(2), 175–178 (1976).
211. Y. Mao and co-workers, *J. Appl. Polym. Sci.* **82**(1), 63–69 (2001).
212. R. Pantani and G. Titomanlio, *J. Appl. Polym. Sci.* **81**, 267–278 (2001).
213. J. Suhm and co-workers, *Acta Polym.* **49**(2/3), 80–87 (1998).
214. MOLDFLOW, Moldflow Australia, Victoria, Australia.
215. C-MOLD, AC Technology, Ithaca, N.Y., IDEAS, Structural Dynamics Research Corp., Cincinnati, Ohio.
216. F. Romani and co-workers, *Polymer* **43**, 1115–1131 (2002).
217. G. Dean and B. Read, *Polym. Test.* **20**, 677–683 (2001).
218. S. Bastida and co-workers, *Polym. Test.* **17**(2), 139–145 (1998).
219. S. Jafari and A. Gupta, *J. Appl. Polym Sci.* **78**, 962–971 (2000).
220. F. Ramsteiner, *Polym. Test.* **18**, 641–647 (1999).
221. A. V. Shenoy and D. R. Saini, *Polym. Test.* **6**(1), 37–45 (1986).
222. W. Grellmann and M. Che, *J. Appl. Polym. Sci.* **66**, 1237–1249 (1997).
223. W. Li, R. Li, and S. Tjong, *Polym. Test.* **16**, 563–574 (1998).
224. S. Seidler and W. Grellmann, *Polym. Test.* **14**, 453–469 (1995).
225. K. Kendall, W. J. Clegg, and R. D. Gregory, *J. Mater. Sci. Lett.* **10**, 671–682 (1991).
226. S. W. Hawley, *RAPRA Rev. Rep.* **5**(12), 14 (1992).
227. J. d'Almeida and S. Monteiro, *Polym. Test.* **18**, 407–414 (1999).
228. F. Ramsteiner and T. Armbrust, *Polym. Test.* **20**, 321–327 (2001).
229. A. Stearn, M. Novotny, and R. Lang, *Polym. Test.* **17**, 403–422 (1998).
230. A. Stearn, M. Novotny, and R. Lang, *Polym. Test.* **17**, 423–441 (1998).
231. F. Ramsteiner, *Polym. Test.* **15**, 573–584 (1996).
232. C. Bernal, P. Montemartini, and P. Frontini, *J. Polym. Sci. Part B* **34**, 1869–1880 (1996).
233. G. C. Adams and co-workers, *Polym. Eng. Sci.* **30**(4), 24–28 (1990).
234. D. B. Barry and O. Delatycki, *J. Appl. Polym. Sci.* **38**, 339–350 (1989).
235. Y.-W. Mai and P. Powell, *J. Polym. Sci., Polym. Phys.* **29**, 785–793 (1991).
236. I. Low, G. Paglia, and C. Shi, *J. Appl. Polym. Sci.* **70**, 2349–2352 (1998).
237. A. Flores and co-workers, *Polymer* **41**, 5431–5435 (2000).
238. S. Fakirov, F. Calleja, and M. Krumova, *J. Polym. Sci. Part B.* **37**, 1413–1419 (1999).
239. C. Xiang and co-workers, *J. Polym. Sci. Part B* **39**(1), 47–59 (2000).
240. R. Brown, *Polym. Test.* **14**, 403–414 (1995).
241. R. J. Roe and C. Gievewski, *Polym. Eng. Sci.* **15**(6), 197 (1975).
242. K. Takahashi, A. E. Abo-El-Ezz, and N. Takeda, *Proceedings of the 7th International Conference*, Cambridge, U.K., 1988, pp. 29/1–29/4.
243. J. Strebel, *Polym. Test.* **14**, 189–202 (1995).
244. E. Moskala, *Polymer* **39**, 675–680 (1998).
245. ISO 4599, Plastics: Determination of Resistance to Environmental Stress-Cracking, Bent Strip Method, ISO, Geneva, Switzerland, 1986.
246. R. P. Brown, ed., *Handbook of Plastics Test Methods*, 3rd ed., John Wiley & Sons, Inc., New York, 1988, p. 354.

247. D. Kiessling and W. Schaaf, *Plast. u. Kaut.* **33**, 310–313 (1986).
248. A. Turnbull, A. Maxwell, and S. Pillai, *Polym. Test.* **19**(2), 117–129 (2000).
249. I. Jakubowica and co-workers, *Polym. Test.* **19**, 729–753 (2000).
250. T. Kobayashi and co-workers, *Kobunshi Ronbun* **42**, 405–413 (1985).
251. J. Boxhammer, *Polym. Test.* **20**, 719–724 (2001).
252. Ref. 246, pp. 271–272.
253. J. M. Garcia and co-workers, *J. Polym. Sci. Part B* **35**, 457–468 (1997).
254. T. R. Manley, J. A. Stonebanks, and P. Laggon, *Polym. Commun.* **28**, 17 (1988).
255. R. Sharma and co-workers, *J. Appl. Polym. Sci.* **68**, 553–560 (1998).
256. A. Bernes and C. Locahanne, in S. E. Keithwath, ed., *Order in the Amorphous State of Polymers*, Plenum Publishing Corp., New York, 1987, p. 305.
257. P. Bartolomeo, J. Chailan and J. Vernet, *J. Polym. Sci. Part B* **38**, 2162–2169 (2000).
258. A. Maxwell, L. Monnerie, and I. Ward, *Polymer* **39**, 6851–6859 (1998).
259. R. Diaz-Calleja, J. De Abajo, and J. de la Campa, *J. Polym. Sci. Part B* **35**, 919–927 (1997).
260. F. Tihminlioglu and co-workers, *J. Polym. Sci. Part B* **35**, 1279–1290 (1997).
261. A. Voelkel and co-workers, *Polymer* **37**, 455–462 (1996).
262. Ref. 246, p. 258.
263. UL 746 A–D, Underwriters Laboratories, Chicago, Ill., 2000/2001.
264. UL 94, Underwriters Laboratories, Chicago, Ill., May 2001.
265. A. Tewarson and R. F. Pion, *Combust. Flame* **26**, 85 (1976).
266. V. Brabraushas, NBSIR 82-2611, U.S. Bureau of Commerce, National Bureau of Standards (now NIST), Washington, D.C., 1982.
267. N. Batho, personal communication, Dark Star Research, Penley, Clwyd, U.K., Mar. 1992.
268. W. N. Reynolds, *RAPRA Rev. Rep.* **3**(2), 30 (1990).
269. A. Sahnoune, F. Massines, and L. Piche, *J. Polym. Sci. Part B* **34**, 341–348 (1996).
270. G. V. Thomas and M. Nair, *J. Appl. Polym. Sci.* **69**, 785–790 (1998).
271. W. N. Reynolds, *RAPRA Rev. Rep.* **3**(2), 30/12 (1990).
272. Y. Bar-Cohen, C. C. Yin, and A. K. Mal, J. Adhesion, **29**, 257–274 (1989).
273. J. Summerscales, ed., *Nondestructive Testing of Fibre-Reinforced Plastic Composites*, Vol. 1, Elsevier Applied Science Publishers, Ltd., Barking, U.K., 1987, pp. 278, 627–629.
274. W. N. Reynolds, *Mat. Des.* **5**/**6**, 256–270 (1985).
275. A. Higuchi and co-workers, *J. Polym. Sci. Part B* **34**, 2153–2160 (1996).
276. I. Linossier and co-workers, *J. Appl. Polym. Sci.* **66**, 2465–2473 (1997).
277. Y. P. Yampolskii and co-workers, *Polymer* **40**, 1745–1752 (1999).
278. B. Wong, Z. Zhang, and Y. Handa, *J. Polym. Sci. Part B* **36**, 2025–2032 (1998).

GENERAL REFERENCES

T. R. Crompton, *Analysis of Polymers, An Introduction*, Pergamon Press, Inc., Oxford, 1989.
D. O. Hummel and A. Solti, *Atlas of Polymer and Plastics Analysis*, Vol. 2, VCH Publishers, New York, 1988.
M. P. Sepe, *Dynamic Mechanical Analysis for Plastics Engineering*, Plastics Design Library, Norwich, New York, 1998.
E. Turi, ed., *Thermal Characterization of Polymeric Materials*, Academic Press, Inc., New York, 1997.
R. P. Brown, ed., *Handbook of Polymer Testing*, Marcel Dekker, New York, 1998.

ASTM Volumes 8.01–8.03, Testing of Plastics, ASTM, Philadelphia, Pa. (published annually).
T. P. Wampler, ed., *Analytical Pyrolysis Handbook*, Marcel Dekker, New York, 1995.
F. A. Bovey and P. A. Miaree, *NMR of Polymers*, Academic Press, New York, 1996.
J. G. Williams, *Fracture Mechanics of Polymers*, John Wiley & Sons, Inc., New York, 1987.

BARBARA J. FURCHES
The Dow Chemical Company

Table 1. **A Survey of Common Thermal Analysis Techniques**[a,b]

Technique	Abbreviation	Property measured (dependent variable)
thermogravimety	TG	mass, m
derivative thermogravimetry	DTG	dm/dt
differential thermal analysis	DTA	dT/dt
differential scanning calorimetry	DSC	dH/dt
thermomechanometry		
thermomechanical analysis	TMA	L, dL/dT
thermal dilatometry	TDA	V, dV/dT
dynamic mechanical analysis (including torsional braid analysis, TBA)	DMA	$G^*(\omega)$
thermoelectrometry		
thermally simulated conductivity	TSC	di/dt
thermally stimulated polarization	TSP	
thermally stimulated depolorization	TSD	
dielectric thermal analysis	DETA	$Z^*(\omega)$
thermophotometry		
thermoluminescence (including oxyluminescence)	TL	dI/dt
thermal microscopy	TM	
emanation thermal analysis	ETA	Radioactive gas evolution
thermosonimetry	TS	Acoustic emission
evolved gas analysis	EGA	GC/MS/IR, etc
thermomagnetometry	TM	Magnetic effect on TG

[a]From Ref. 127.

[b]Combined simultaneous techniques—many of these techniques can be combined to give simultaneous or sequential measurements on the same sample, eg, TG/MS, TG/IR, DSC/XDR, DSC/TG/MS, pyrolysis/GC, Differential photocalorimetry (DPC), etc.

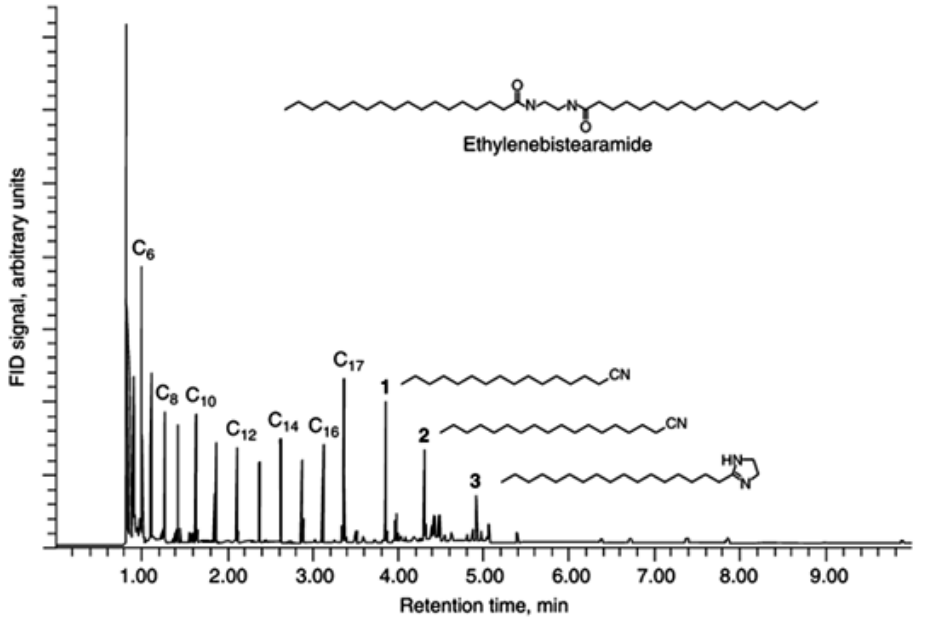

Fig. 1. The pyrogram of *N*,*N*′-ethylenebistearamide. The identification of peaks labeled in the pyrogram is 1 – hexadecanenitrile, 2 – octadecanenitrile, 3 – 1*H*-2-heptadecyl-4,5-dihydroimidazole. (Reprinted from Ref. 67, Copyright (2000), with permission from Elsevier Science.)

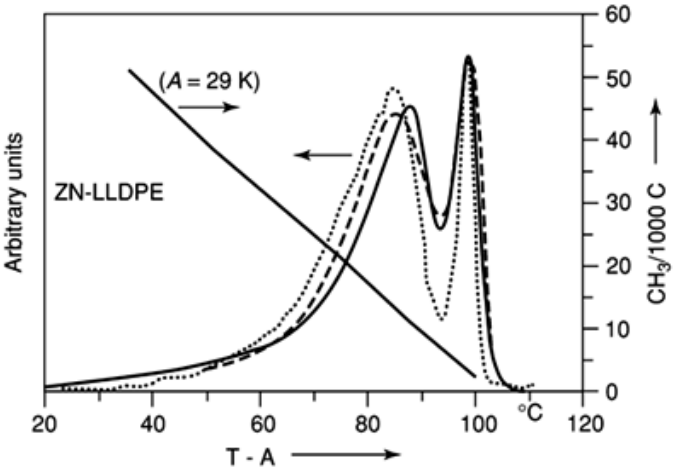

Fig. 2. Comparison of the short-chain branching distribution of ZN-LLDPE as obtained by TREE, CRYSTAF, and DSC. A calibration curve for the DSC data is plotted on the right axis. (Reprinted from Ref. 101, Copyright (2000), with permission from Elsevier Science.)

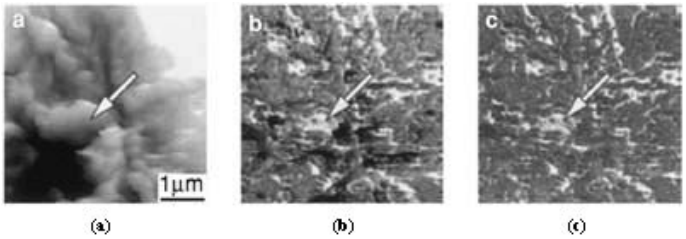

Fig. 3. (**a**) Topography, (**b**) amplitude (∼elasticity), and (**c**) phase (∼viscoelasticity) simultaneously acquired images of PES/SAN. The scale bar applies to all three images. (Reprinted from Ref. 125, Copyright (2001), with permission from Elsevier Science.)

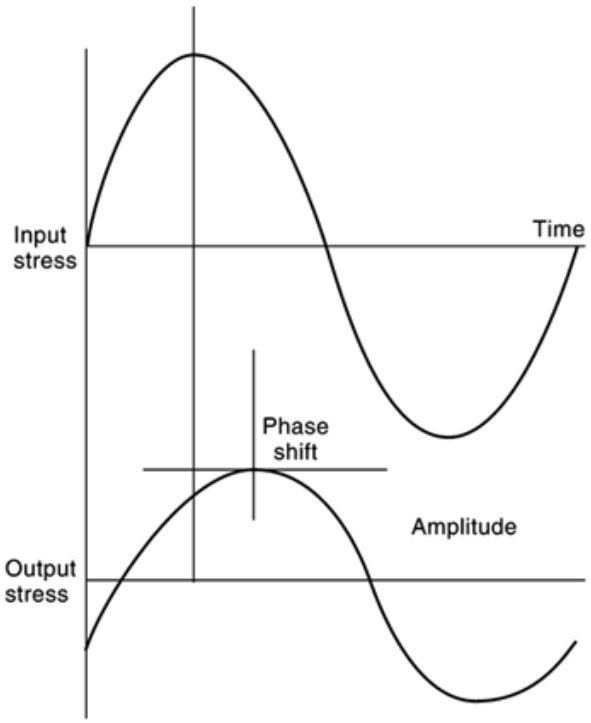

Fig. 4. Applied stress and resultant strain in DMA measurements.

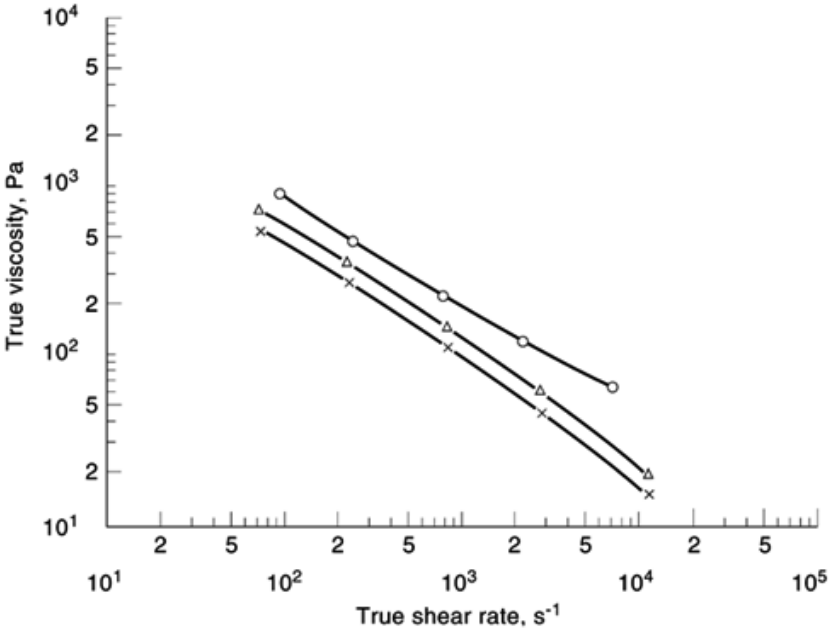

Fig. 5. Capillary melt viscosity; ○, = 300°C, △, = 320°C, and ×, = 340°C. (Courtesy of The Dow Chemical Company.)

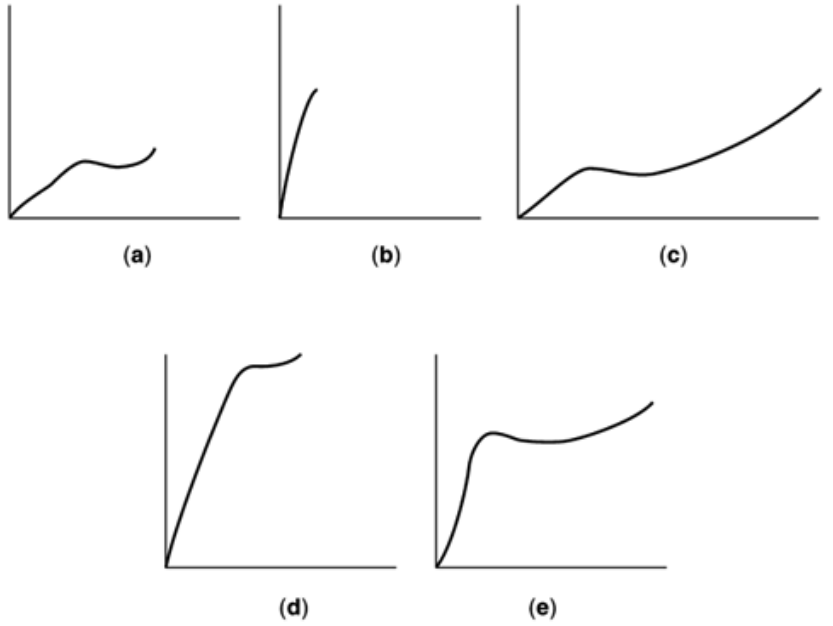

Fig. 6. Types of stress–strain curves: (**a**) soft and weak; (**b**) hard and brittle; (**c**) soft and tough; (**d**) hard and strong; and (**e**) hard and tough.

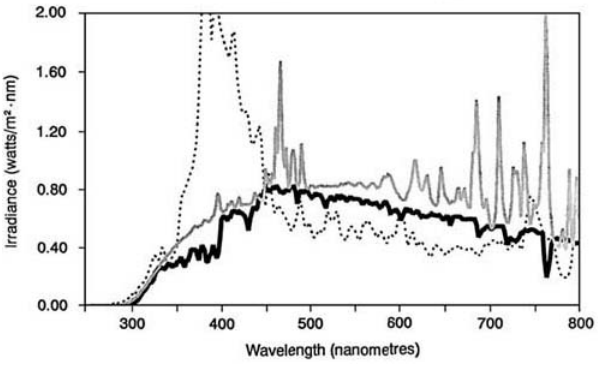

Fig. 7. Comparison of xenon arc, sunshine carbon arc, and Miami average 45°S daylight, where (▒▒▒) represents xenon with Type S high borate filters, 0.35 W/(m^2·nm) at 340 nm; (···) represents sunshine carbon arc with Corex; and (▬) represents daylight. (Courtesy of Atlas Electric Devices Co.)